Neuron, Volume *76*

Supplemental Information

NGL-2 Regulates Input-Specific Synapse Development in CA1 Pyramidal Neurons

Laura A. DeNardo, Joris de Wit, Stefanie Otto-Hitt, and Anirvan Ghosh

Figure S1 (Related to Figure 1)

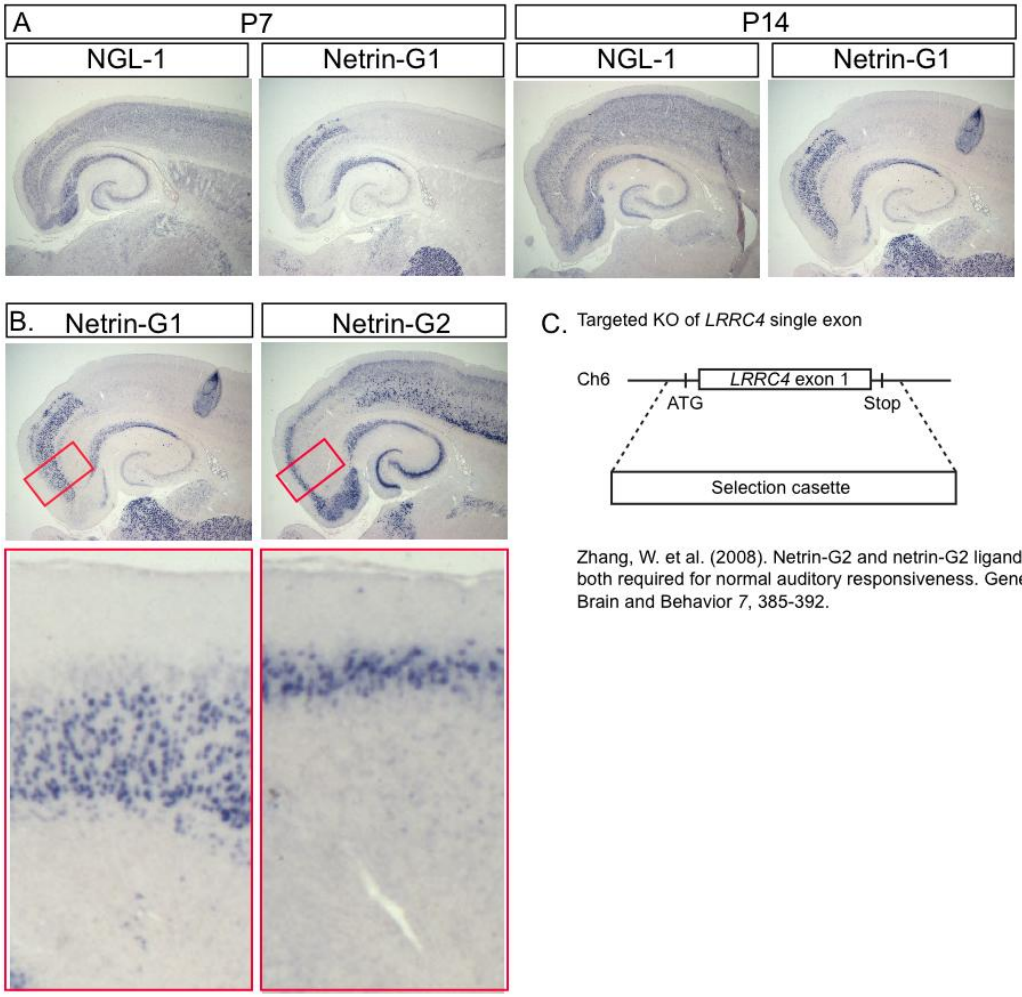

Zhang, W. et al. (2008). Netrin-G2 and netrin-G2 ligand are both required for normal auditory responsiveness. Genes, Brain and Behavior 7, 385-392.

Figure S1 (Related to Figure 1). NGL1 in situ patterns and schematic of generation of NGL-2 knockout mice

(A) In situ hybridizations with antisense NGL-1 and Netrin-G1 probes in horizontal sections from P7 (left) and P14 (right) rat brain. (B) Comparison of Netrin-G1 and Netrin-G2 in situ patterns. Red boxes outline entorhinal cortex. Zoomed views illustrate that Netrin-G1 is selectively expressed in layer 3 and Netrin-G2 is selectively expressed in layer 2. (C) Schematic of targeting strategy used to generate NGL-2 (*Lrrc4*) knockout mice as part of a collaboration between Lexicon Pharmaceuticals and Genentech. Targeting vectors were generated using the lambda knockout system. A yeast selection cassette was generated using the polymerase chain reaction and introduced into the genomic clone by recombination in yeast, and used to target and excise the single exon of *Lrrc4* (Zhang et al., 2008).

Figure S2 (Related to Figure 4)

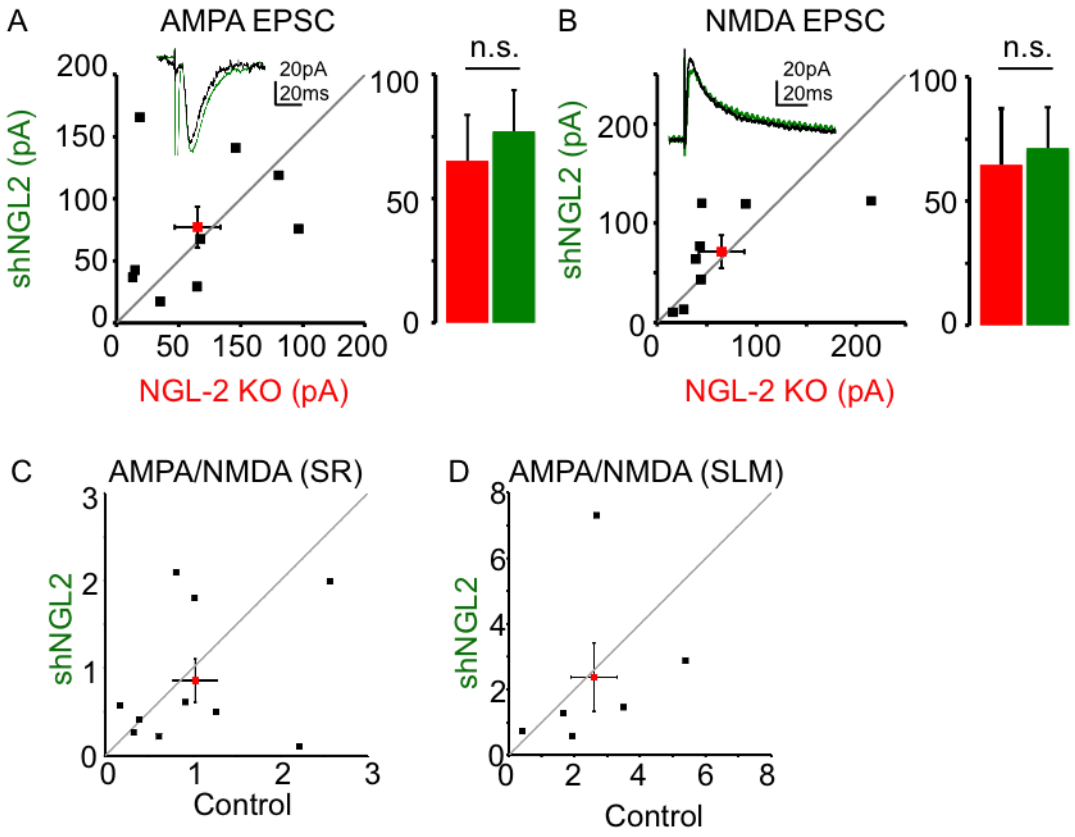

Figure S2 (Related to Figure 4). shNGL2 does not affect the ratio of AMPAR- to NMDAR-mediated currents nor does it have any effect in an NGL2 KO background

(A) shNGL2 has no effect on the amplitude of AMPAR EPSCs in the NGL-2 KO mouse (Control: 65.19±16.72, n=9; shNGL2: 77.15±17.64, n=9; p=0.57, paired t-test) (B) shNGL2 has no effect on the amplitude of NMDAR EPSCs in the NGL-2 KO mouse (Control: 64.59±22.77, n=8; shNGL2: 71.27±16.51, n=8; p=0.60, paired t-test). Summary statistics represent mean±SEM. (C) shNGL2 has no effect on the AMPA/NMDA ratio at SR synapses (Control 1.02±0.25, n=10; shNGL2 0.85±0.24, n=10; p=0.58, student's t-test). (D) shNGL2 has no effect on the AMPA/NMDA ratio at SLM synapses (Control 2.59±0.69, n=6; shNGL2 2.37±1.04, n=6; p=0.84, student's t-test).

Figure S3 (Related to Figure 5)

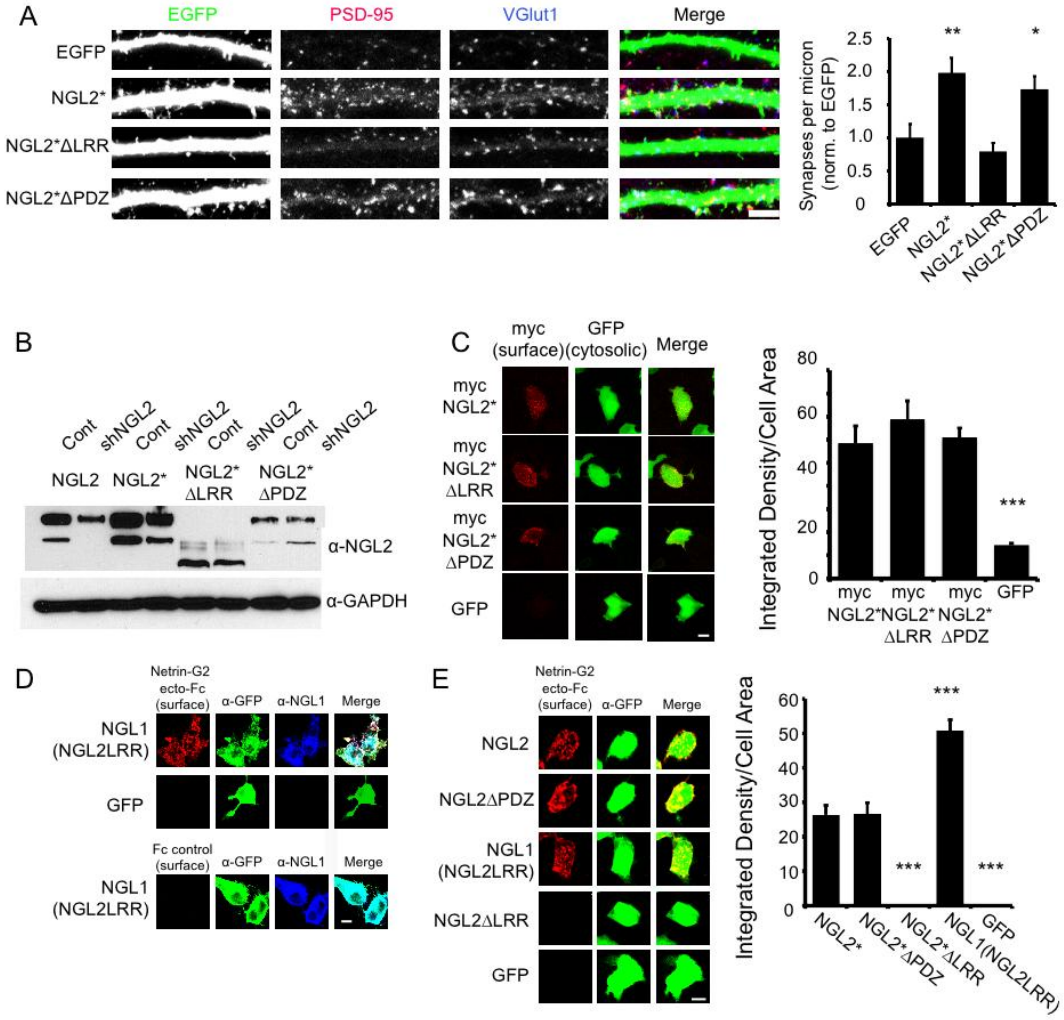

Figure S3 (Related to Figure 5). Characterization of NGL mutant proteins

(A) Overexpression of NGL2* and NGL2*ΔPDZ caused a significant increase but NGL2*ΔLRR did not affect synapse density in cultured hippocampal neurons (EGFP: 1.00±0.20, n=18 NGL2*:1.98±0.23, n=18; NGL2*ΔLRR: 0.79±12, n=17; NGL2*ΔPDZ: 1.73±0.19, n=19; one-way ANOVA, $p<0.0001$. Post-hoc Tukey Test *$p<0.05$, **$p<0.01$. Scale bar = 10 μm). (B) shRNA-resistant NGL-2 domain deletion constructs (Figure 6D) were co-expressed with either control or shNGL2 plasmids in HEK293T cells and NGL-2 content in lysates was analyzed by western blot. (C) Myc tagged constructs shown in A were expressed in HEK293T cells along with cytosolic GFP. Cells were live labeled with a mouse anti-myc antibody and then fixed, permeabilized, stained for GFP and then imaged on a confocal micrscope. Scale bar is 10μm. Quantified intensity of surface labeling normalized to cell area showed no difference between mutants, but all three were significantly above control levels (NGL2*=58±7.50, NGL2*ΔLRR=68.83±7.94, NGL2*ΔPDZ=60.96±4.02, GFP=14.46±0.68, $p<0.0001$, one-way ANOVA, $p<0.001$ for all mutants compared to GFP, no significant differences between mutants, Tukey-Kramer Test *$p<0.05$, **$p<0.01$). (D) NGL1(NGL2LRR) or GFP were expressed in HEK293T cells. Cells were live labeled with a Netrin-G2 ecto-Fc and then fixed, permeabilized, stained for GFP and NGL1 and then imaged on a confocal micrscope. Scale bar is 10μm. (E) NGL2, NGL2ΔLRR, NGL2ΔPDZ, NGL1(NGL2LRR) or GFP control were expressed in HEK293T cells along with cytosolic GFP. Cells were live labeled with a Netrin-G2 ecto Fc fusion protein and imaged with a confocal miscroscope. Scale bar is 10μm. Quantified intensity of surface labeling normalized to cell area (NGL2: 26.39±2.66, n=31; NGL2ΔPDZ: 26.67±3.19, n=27; NGL2ΔLRR: 0.03±0.002, n=32; NGL1(NGL2LRR): 50.87±2.98, n=20; GFP: 0.03±0.002, n=15; $p<0.0001$ one-way ANOVA, post hoc Tukey test shown on graph. ***$p<0.001$). Summary statistics reported as mean±SEM.

Figure S4 (Related to Figure 7)

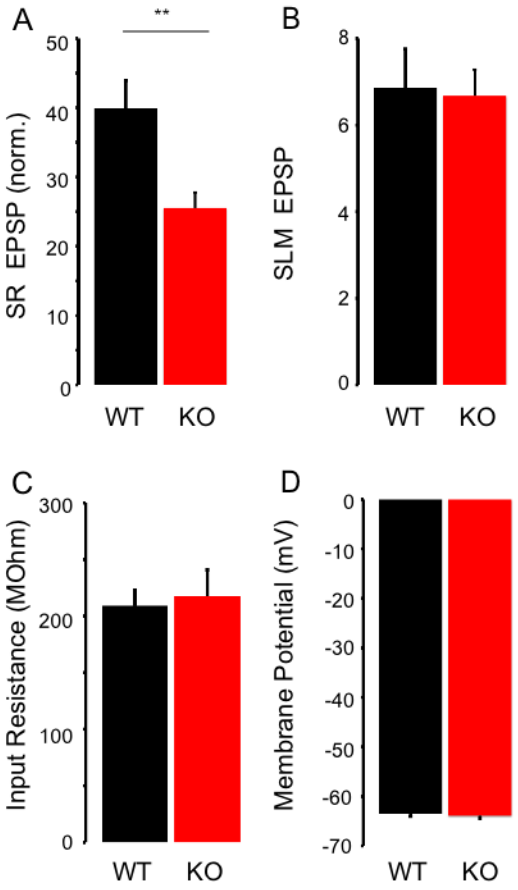

Figure S4 (Related to Figure 7). The relative amplitude of SR EPSPs is reduced in NGL-2 KO mice

(A) SR EPSP normalized to the SR fiber volley amplitude was reduced in NGL-2 KO mice. (SC normalized EPSP: WT=39.96±3.97, n=15; KO=25.56±2.22, n=19; p=<0.001, student's t-test). (B) Peak SLM EPSP was between WT and KO mice (SLM peak EPSP: WT=6.85±0.89 mV, n=15; KO=6.67±0.61 mV, n=19; p=0.61, student's t-test). (C) Input resistance was not significantly different between WT and KO mice (R_{in}: WT=209.14 MΩ, n=15; KO=217.64 MΩ, n=19; p=0.76, student's t-test). (D) Resting membrane potential was not significantly different between WT and KO animals (V_m: WT= -63.57±0.49 mV, n=15; KO= -63.88±0.51 mV, n=19; p=0.39, student's t-test). All summary statistics reported as mean±SEM.

Table S1 (Related to Figure 5)

Tukey-Kramer Multiple Comparisons

	shNGL2	shNGL2 NGL2*	shNGL2 NGL2* ΔLRR	shNGL2 NGL2* ΔPDZ	shNGL2 NGL1 r123
Cont.	**	n.s.	*	**	n.s.
shNGL2		***	n.s.	n.s.	***
shNGL2 NGL2*			***	***	n.s.
shNGL2 NGL2 *ΔLRR				n.s.	***
shNGL2 NGL2 *ΔPDZ					***
shNGL2 NGL1 r123					

*p<0.05, **p<0.01, ***p<0.001, n.s. not significant

Table S1 (Related to Figure 5).

Complete results of the posthoc Tukey-Kramer multiple comparisons test from the one-way ANOVA performed to analyze CA1 spine density in control, knockdown and rescue conditions (Figure 5). *p<0.5, **p<0.01, ***p<0.001.

Supplemental Experimental Procedures

Hippocampal Culture and Transfections

Hippocampal neurons were cultured from P0 Long-Evans rats (Charles River, Wilmington, MA) and plated on poly-D-lysine (Millipore, Temecula, CA), and laminin (Invitrogen, Carlsbad, CA) coated chamber slides (Nalge Nunc International, Rochester, NY). Neurons were maintained in Neurobasal-A medium (Invitrogen) supplemented with B27, glucose, glutamax, penicillin/streptomycin (Invitrogen) and 25 μM β-mercaptoethanol. Neurons were transfected using calcium phosphate at 7 DIV.

Immunocytochemistry in neurons

At DIV 14, neurons were fixed in 4% paraformaldehyde, 4% sucrose in phosphate buffered saline (PBS) and processed for immunofluorescence according to standard procedures. Primary antibodies were: goat anti-GFP (Abcam, Cambridge, MA); guinea pig anti-VGlut1; mouse anti-PSD-95 (Thermo Scientific); Fluorophore-conjugated secondary antibodies were from Jackson ImmunoResearch (West Grove, PA) or Invitrogen.

Immunocytochemistry in HEK293T cells

HEK293T cells were co-transfected with pEF-BOS mycNGL constructs and pEF-BOS GFP as a cytosolic fill using Fugene6 (Roche). After 24 hours, standard media was replaced with Optimem (GIBCO). Several hours later, mouse anti-myc (Santa Cruz) or Netrin-G2 ecto-Fc was diluted 1:500 in DMEM (GIBCO) with 20mM HEPES and added to the cells for 30 minutes at room temperature. Cells were then fixed in 4% PFA and 4% sucrose in PBS and blocked with 3% BSA and 0.2% Triton-X 100 in PBS. Cells were incubated with goat anti-GFP (Abcam) overnight at 4°C. Fluorophore-conjugated secondary antibodies (Invitrogen) were used at 1:1000.

Image Acquisition and Analysis

Images were captured on a Leica SP5 confocal microscope (Leica Microsystems, Bannockburn, IL). Z-stacks were collapsed in a maximum projection and integrated density per cell area was analyzed using ImageJ software.

In Situ Hybridization

Briefly, digoxigenin-labeled cRNA probes were generated from linearized cDNA templates: The entire coding regions of mouse NGL2 and Netrin-G2a (gift from Dr. Eunjoon Kim, KAIST) were subcloned in a reverse orientation in pcDNA3.1(+)B and pcDNA3.1(-) (Invitrogen, Carslbad, CA) respectively, to generate antisense riboprobes from the entire coding sequence using T7 polymerase. Control sense probes yielded no specific signal (data not shown).

Immunohistochemistry

To label neuronal markers, sections were probed with mouse anti-NeuN (Chemicon International, Inc, Temecula, CA), or with chicken anti-Neurofilament (Abcam) and mouse anti-MAP2 (Sigma) antibodies diluted 1:1000 in blocking solution overnight at 4°C. Sections were washed three times with blocking solution, then probed with fluorophore-conjugated fluorescent secondary antibodies (Invitrogen) diluted 1:1000 in blocking solution for one hour at room temperature. Sections were washed three times with PBS and then mounted on slides using Fluoromount-G from Southern Biotech (Birmingham, AL).

Electrophysiology

Responses were evoked by stimulating each pathway with a platinum 2-contact cluster electrode (FHC) 100-200 microns lateral to the recording site. For fEPSP and whole cell voltage clamp experiments, analysis was usually based on the average of 15 sweeps. CA1 pyramidal cells were visualized by infrared differential interference microscopy (Olympus BX51WI). To measure AMPAR-mediated currents, cells were voltage clamped at -70mV and the peak response was measured. To measure the NMDAR-mediated current, cells were depolarized to +40mV and analyzed as the mean of a 10 ms window measured at 50ms after the stimulus artifact, by which time the fast AMPA component had decayed and the remaining response could be attributed to NMDAR-mediated currents.

There was no difference in R_s or R_{in} between conditions in any experiments. Short term facilitation experiments: (R_s: WT=17.70±0.86 MΩ, n=28; KO=19.31±0.96 MΩ, n=21; n.s.; student's t-test; R_{in}: WT=404.58±150.97 MΩ, n=28; KO=330.00±34.59 MΩ, n=21; n.s.; student's t-test). AMPA/NMDA ratio experiments: (R_s: WT=17.94±0.90 MΩ, n=21; KO=18.01±0.77 MΩ, n=19; n.s., student's t-test; R_{in}: WT=556.19±55.72 MΩ, n=21; KO=499.00±32.95 MΩ, n=19; n.s., student's t-test). shNGL2 recordings in WT animals (R_s: Control=19.04±1.22 MΩ, n=19; shNGL2=17.51±0.19 MΩ, n=19; p=0.19, paired student's t-test; R_{in}: Control=447. 98±95.72 MΩ, n=19; shNGL2=383.14±49.83 MΩ, n=19; p=0.51, paired student's t-test). shNGL2 recordings in NGL-2 KO animals (R_s: Control=19.05±3.46 MΩ, n=9; shNGL2=20.60±3.08 MΩ, n=9; p=0.68, paired t-test; R_{in}: Control=512.05±59.04, n=9; shNGL2=438.61±80.13, n=9; p=0.29, paired t-test). For mEPSC recordings, cells were voltage clamped at -70mV in the presence of 0.5 uM Tetrodotoxin (Tocris) and mEPSCs were detected by fitting to a variable amplitude template using pClamp10 analysis software. The peak current of each mEPSC was calculated. Average mEPSC amplitude and inter-event-interval was calculated for each cell and then averaged across each condition to determine the population mean and SEM. R_s and R_{in} did not differ between conditions in mEPSC recordings: (R_s: WT=18.92±1.63 MΩ, n=19; KO=18.09±1.98 MΩ, n=13; n.s., student's t-test; R_{in}: WT=386.95±24.55 MΩ, n=19; KO=361.24±45.77 MΩ, n=13; n.s., student's t-test). Cells were excluded if R_s varied by more than 20% during a recording. Summary statistics represent mean±SEM.

Quantitative PCR

For analysis of cDNA levels, primers were designed around exon/intron boundaries using NCBI Primer Blast. PCR was run using the following cycling conditions: 95°C/10 min; 95°C/15 s and 57°C/1 min for 40 cycles. Primers used were as follows; GAPDH forward GGGGGCTCTCT GCTCCTCCC, reverse CAGGCGTCCGATACGGCCAA; EphB2 forward AGAAGCTGGTACGAATGGGAGAAGT, reverse CCCTGCGAATAAGGCCACTTCGG; NGL1

forward CGTTGCCTATTTACTGCATAGAGAC, reverse GTTAAACCTAGGACCTATCATTATCTGC; NGL2 forward ACTGTGCCAAAAGGTTGAGAGGCA, reverse TGCACATGTACAAAGAAACAGCCCC; NGL3 forward GCTACCTGAACTTGCAAGAGAAC, reverse GAGTTCCAGTGTGTTGAGACTG.

In utero electroporation

For spine analysis, we electroporated pFCK0.4(GW), pFCK0.4(GW)shNGL2, or a combination of pFCK0.4(GW)shNGL2 plus pEF-BOS-NGL2*, pEF-BOS-NGL2*ΔLRR, or pEF-BOS-NGL2*ΔPDZ. For electrophysiology, pFCK(0.4)GW or pFCK(0.4)GW shNGL2 was mixed with PBS and 0.01% Fast Green. For NGL2 localization, pEF-BOS-NGL2-GFP was mixed with pCAG-tdTomato along with PBS and 0.01% Fast Green.

Lentivirus production

For lentivirus production, 293T cells were transfected with FCK(0.4)GW control or FCK(0.4)GW-shNGL2 plasmids and helper plasmids MDL, RSV-REV and VSVG using Polyethylenimine (PEI) transfection agent (Fischer Scientific). Supernatant was collected 48 hrs after transfection, spun at 2000 rpm to remove debris and filtered through a 0.22 µm filter (Millipore). Viral particles were pelleted using two centrifugation steps at 19500 rpm for 2 hrs each. The final pellet was resuspended in 100 µl PBS and stored at -80°C in 10 µl aliquots.

Lentiviral Infection of Neurons

To measure the effect of NGL-2 knockdown on endogenous NGL-2 levels, dissociated rat cortical neurons were grown at high density in poly-D-lysine/laminin coated 12 well plates and infected with control or shNGL-2 lentivirus at DIV 5. Approximately 80% of neurons were infected based on EGFP expression.

Imaging and analysis of dendritic spines from electroporated animals

Fixed sections from electroporated animals were immunostained with a goat polyclonal anti-

GFP primary antibody (1:3000 dilution; Abcam) and an Alexa 488-conjugated donkey anti-goat secondary antibody (1:1000; Invitrogen). The secondary apical dendrites of CA1 pyramidal neurons were imaged on an Olympus FV300 confocal microscope. Dendritic protrusions were counted in Z-stacks in NIH ImageJ and the length of dendritic segments measured with the Simple Neurite Tracer plug-in blind to transfection condition.

In vivo Postnatal Viral Injection

NGL-2 KO mice were injected on the day after birth with concentrated shNGL2-CamKII-GFP lentivirus solution (10^{12} pfu). Newborns were anesthetized on ice and then stabilized in a custom mold before being injected with 69 nl of viral solution at six sites targeting the hippocampus intracerebrally using Nanoject (Drummond Scientific) and a beveled glass injection pipette. Animals recovered immediately after injection and were used for recording 13–15 days afterward.

Supplemental References

Zhang, W., Rajan, I., Savelieva, K.V,. Wang, C-Y., Vogel, P., Kelly, M., Xu, N., Hasson, B., Jarman, W., and Lanthorn, T.H. (2008). Netrin-G2 and netrin-G2 ligand are both required for normal auditory responsiveness. Genes, Brain and Behavior *7*, 385-392.